Gene amplification of ESR1 in breast cancers-fact or fiction? A fluorescence in situ hybridization and multiplex ligation-dependent probe amplification study

著者	Ooi Akishi, Inokuchi Masafumi, Harada Shinichi, Inazawa Johji, Tajiri Ryousuke, Sawada-Kitamura Seiko, Ikeda Hiroko, Kawashima Hiroko, Dobashi Yoh
journal or publication title	Journal of Pathology
volume	227
number	1
page range	8-16
year	2012-05-01
URL	http://hdl.handle.net/2297/30345

Gene amplification of *ESR1* in breast cancers - Fact or fiction? A fluorescence *in situ* hybridization and multiplex ligation-dependent probe amplification study.

Running title: Gene amplification of *ESR1* in breast cancers

Akishi Ooi [1, 4)], Masafumi Inokuchi [2)], Shinichi Harada [3)], Johji Inazawa [4)], Ryousuke Tajiri [1)], Seiko Sawada-Kitamura [5)], Hiroko Ikeda [5)], Hiroko Kawashima [6)], Yoh Dobashi [7)]

[1] Department of Molecular and Cellular Pathology and [2] Department of Breast Oncology, Division of Cancer Medicine, and [3] Center for Biomedical and Research Education, Graduate School of Medical Science, Kanazawa University, Ishikawa 920-8641, Japan
[4] Department of Molecular Cytogenetics, Medical Research Institute, Tokyo Medical and Dental University, Tokyo 113-8510, Japan
[5] Pathology Section and [6] Section of Breast Oncology, University Hospital, Kanazawa University, Ishikawa 920-8641, Japan
[7] Department of Pathology, Saitama Medical Center, Jichi Medical University, Saitama 330-8503, Japan

Corresponding author. Akishi Ooi, MD, PhD, Department of Molecular and Cellular Pathology, Kanazawa University, 13-1 Takara-machi, Kanazawa, Ishikawa 920-8640, Japan. E-mail: aooi@med.kanazawa-u.ac.jp

Conflict of interest: No conflicts of interests are declared.

Word count (intro-discuss): 3,683 words

Abstract

Estrogen receptor-alpha (ERα), encoded by the *ESR1* gene located on 6q25, is a nuclear transcription factor. Since it was reported in 2007 that more than 20% of breast cancers show *ESR1* gene amplification, there has been considerable controversy about its frequency and clinical significance. The aim of this study was to assess the real and exact frequency and levels of *ESR1* amplification in breast cancers. In a total of 106 breast needle biopsy specimens examined by immunohistochemistry, 78 tumors contained more than 10% ERα-positive cancer cells. In fluorescence *in situ* hybridization (FISH) analysis with an *ESR1*-specific probe, variously extended *ESR1* signals were found in ERα-expressing cells. Some of these were indistinguishable from large clustered signals generally accepted to mean high-level gene amplification in homogeneously staining regions (HSR), and could be considered to represent gene amplification. However, with RNase treatment, the 'HSR-like' signals changed to small compact signals, and are thus thought to represent concentrated RNA. FISH using two differently labeled probes corresponding to the non-overlapping 5' and 3'-end portions of the *ESR1* gene on imprinted cells showed a preserved spatial relationship of the 3' to 5' sequence of *ESR1*, therefore strongly suggesting that the RNA consisted of primary transcripts. Using imprinted cells obtained by 51 fresh tumors, precise enumeration of *ESR1* signals with a correction by the number of centromere 6 on FISH after RNase A treatment revealed that three tumors (5.9%) had tumor cells with one to three additional copies of *ESR1* as predominant subpopulations. This infrequent and low level of gene amplification of *ESR1* was also detected as a 'gain' of the gene by analysis with multiplex ligation-dependent probe amplification (MLPA). We believe that these consistent results from immunohistochemistry, FISH, and MLPA in the present study settle the long-standing debate concerning gene amplification of *ESR1* in breast carcinoma.

Key words: *ESR1*, FISH, MLPA, ERα, gene amplification, breast cancer

Introduction

Estrogen receptor-alpha (ERα) is as a nuclear transcription factor activated by estrogen to regulate the growth and differentiation of normal breast epithelial cells. These pathways remain operative to varying degrees in breast cancers, and thus ERα is a target for various endocrine therapies [1, 2]. ERα is encoded by the estrogen receptor-alpha gene (*ESR1*) located on 6q25. In 2007, Holst et al. [3] reported that more than 20% of breast cancers showed *ESR1* gene amplification, mainly based on FISH results using tissue microarrays. Furthermore, they suggested that the amplification of *ESR1* is a frequent mechanism for ERα overexpression, and that the amplification was significantly correlated to the response to anti-estrogen therapy. However, this was immediately disputed by other groups of researchers, because first, other FISH and chromogen *in situ* hybridization (CISH) studies using tissue microarrays [4, 5] detected amplification in less than 1.5% of breast cancers, and second, DNA extraction methods such as array comparative genomic hybridization (CGH) and quantitative PCR consistently detected very low frequencies (less than 3%) or no amplification [4, 6, 7]. Since then, there has been heated discussion about the frequency and clinical significance of *ESR1* amplification [8-10]. Recently, Moelans et al. also examined *ESR1* amplification of breast carcinomas using multiplex ligation-dependent probe amplification (MLPA), and found that its amplification is rare and has poor concordance with the amplification detected by FISH and overexpression of ERα [11].

The major cause of the discordance between FISH and CISH studies might be the use of different (an automated or manual) scoring systems and/or different interpretations of the definition of ‘amplification’. The used samples also could be another cause, because tissue microarrays used in previous FISH studies were made from isolated surgical specimens in which the size of each specimen was too small to observe background lesions or possible cancer heterogeneity. Furthermore, it is technically difficult to optimize FISH conditions for each specimen in an array [5], and after the introduction of neo-adjuvant therapy, surgical materials may have therapeutic effects. MLPA is a new, high-resolution method for detecting copy number variations in genomic sequences [12]. Moelans et al. have shown high concordance between the *ERBB2* status of breast cancers detected by MLPA, CGH, FISH, and immunohistochemistry (IHC) [13]. Thus,

in the present study, we performed FISH using whole sections of core needle biopsy specimens that were carefully fixed and processed to optimize FISH results, as well as imprinted cells obtained from fresh surgical specimens. In addition, we analyzed gene amplification by MLPA and compared the results with FISH results. In order to test the validity of the methodology, *ERBB2* status was also examined by IHC, FISH, and MLPA.

Materials and Methods

Core needle biopsies, touch smears, and DNA samples

Core needle biopsy specimens obtained from 106 breast carcinomas were immediately fixed in 10% buffered formalin for no longer than overnight and embedded in paraffin according to standard procedures. Serial sections (4 μm) placed onto MAS-coated glass slides™ (Matsunami, Tokyo, Japan) were used for hematoxylin-eosin staining, IHC detection of ERα and ERBB2, and FISH analysis. The tumors consisted of 14 ductal carcinomas *in situ*, 87 invasive ductal carcinomas, and 5 invasive lobular carcinomas. Two patients had bilateral cancers. From surgery on 49 patients, small fragments of cancer tissue (51) and adjacent non-neoplastic tissues (37) were trimmed. The cancer tissues were touched on MAS-coated slides™, which were dried and fixed immediately in metacarn solution (methanol/acetic acid, 3:1) and stored in a freezer until FISH analysis. From the rest of the fresh samples, high molecular weight DNA was prepared by protease K (Boehringer Mannheim, Mannheim, Germany) digestion and phenol/chloroform extraction as described elsewhere [14] and used for MLPA analysis. This laboratory study was approved by the Institutional Review Board at the Kanazawa University Hospital (Approval No. 181), and written informed consent was obtained from all patients.

Cell lines and normal lymphocytes

The breast cancer cell line MCF-7 expressing ERα, and cell lines UACC-812 and MDA-361 that do not express ERα [15], were obtained from the American Type Culture Collection (Rockville, MD, USA). Cell lines were grown in RPMI supplemented with 10% fetal bovine serum. The cells were fixed in metacarn solution and dropped on

MAS-coated slides™. Metaphase spreads of normal lymphocytes were purchased from Abbott Laboratories (Abbott Park, IL, USA).

IHC

Monoclonal antibodies against human ERα (clone 6F11, Novocastra, Newcastle upon Tyne, UK; working dilution of 1:50), and a polyclonal antibody against the internal domain of the human ERBB2 (Nichirei, Tokyo, Japan; dilution, 1:100) were used. Antibodies were visualized by avidin-biotin binding to peroxidase-conjugated secondary antibodies (DAKO A/S, Glostrup, Denmark). For evaluations of ERα-staining, only nuclear immunostaining significantly higher than that of stromal cells was considered as positive. ERα positivity was defined as 10% or more positively stained cells per 10 high-power fields according to the recommendation by the Eighth Annual International Expert Consensus Panel on the primary therapy for early cancer in St. Gallen, Switzerland [16]. For the evaluation of ERBB2 positivity, each tumor was scored using the four-tier system recommended by the American Society of Clinical Oncology (ASCO) for IHC of ERBB2 [17] and reviewed by two of the authors.

FISH

We performed FISH analysis of gene amplification of *ESR1* on core needle biopsies, imprinted cancer cells, and cultured cells using *ESR1*-specific bacterial artificial chromosomal (BAC) probe RP11-450E24, which was the same probe used by Holst et al. [3] by labeling with SpectrumOrange™ (Abbott). In order to standardize the chromosome number, a SpectrumGreen™-labeled pericentromeric probe (CEP6™, Abbott), which was specific to centromere 6, was cohybridized.

Tumors with 2+ or 3+ staining by IHC examination of ERBB2 were also further analyzed for *ERBB2* amplification by FISH. This was done using the SpectrumOrange™-labeled *ERBB2* locus (17q12) specific probe, RP11-62N23, and the SpectrumGreen™-labeled pericentromeric 17 probe (CEP17™, Abbott). BAC probes were acquired from BACPAC Resources (Oakland, CA, USA). Our FISH probes contained *E. coli* tRNA in addition to human placental DNA, and Cot-1 DNA as a competitor nucleic acid sequence.

First, we performed FISH using formalin-fixed paraffin-embedded (FFPE) tissues and

imprinted cells with standard methods as described elsewhere [18] without using RNase A digestion. The FISH protocols for imprinted cancer and cultured cells were the same as for FFPE tissues, except protein digestion was made by 0.25 mg/ml pepsin at 37°C for 10 min, and prehybridization fixation was by 1% formaldehyde at room temperature for 5 min. Second, FISH with RNase A treatment was performed by incubating slides with RNase A (100 micro g/ml in 2XSSC) at 37°C for 30 min before hybridization. When necessary, imprinted cells or tissue sections were submitted to digestion with RNase A or with 1U/ml of DNase I for 10 min at 37°C after the first standard FISH [19].

The specimens were counterstained with 4',6-diamidine-2'-phenylindole dihydrochloride and p-phenylenediamine in phosphate-buffered saline and glycerol (DAPI II™) (Abbott) and examined under a fluorescence microscope (Olympus, Tokyo, Japan) equipped with a Triple Bandpass Filter™ set and single Bandpass Filter™ sets (Abbott) to discriminate DAPI II, SpectrumOrange™, and SpectrumGreen™. FISH results were scored manually and gene amplification was determined according to the American Society of Clinical Oncology (ASCO)-approved criteria of *ERBB2* amplification: gene signals/centromere signals > 2.2, definite; 1.8-2.2, equivocal [17]. In addition, gene signals arranged in aggregates, a characteristic of amplified genes located in homogeneous staining regions (HSR) of a chromosome ('HSR-type' signals), as discussed later, were interpreted as positive for amplification. All FISH analyses were performed with observers blinded to the results of the IHC and MLPA analyses. FISH images were taken using a charge coupled device camera and recorded on a personal computer.

MLPA

MLPA analysis was performed using a kit (SALSA MLPA KIT P078-B1 Breast Tumour) from MRC-Holland (Amsterdam, The Netherlands). This kit contains 39 probes for 10 different genes, including two probes for *ESR1* and four probes for *ERBB2*. In addition, 11 reference probes are included in this probe mix, detecting 11 different autosomal chromosomal locations that are relatively quiet in breast tumors.

The MLPA PCR products were separated on an ABI-310 capillary sequencer (Applied Biosystems, Foster City, CA, USA) and interpreted using Genmapper software (Applied Biosystems). Data analysis was performed with Coffalyser MLPA-DAT software (version 9.4, MRC-Holland) generating normalized peak values. Peak values below 0.7 were defined as lost, between 0.7 and 1.3 as normal, between 1.3 and 2.0 as gain, and values > 2.0 as amplified as previously established [11, 12, 20].

Results

IHC

Seventy-eight of a total of 106 cases (74%) were ERα-positive, and 28 (26%) cases were negative. The populations of positive cells in each tumor were more than 80% in 64 tumors and 10-80% in 14 tumors. There were no significant differences between the positive frequencies of DCIS (71%, 10/14), IDC (75%, 65/87), and ILC (60%, 3/5). In non-cancerous breast tissues, ERα staining was found heterogeneously in ductal and acinal cells ranging from 2 to 30%. ERBB2 overexpression was found in 27 tumors (12 of 2+ and 15 of 3+ tumors).

FISH

RP11-450E24 /CEP6™

The RP11-450E24 probe detected its target focus as symmetrical double red spots on chromosome 6 in metaphase chromosomes of normal lymphocytes (Figure 1A). Most interphase nuclei of MCF-7 had four centromere 6-specific signals, indicating tetrasomy 6, and those of UACC-812 and MDA-361 had three signals, indicating trisomy 6 (Figures 1B-D). Usually, orange *ESR1* signals are smaller than the green centromeric 6 signals in UACC-812, MDA-361, and normal lymphocytes; however, nuclei of MCF-7 showed one or two large extended signals of RP11-450E24 corresponding to "HSR-type" signals, suggesting gene amplification in HSR [21, 22], although HSR was not found in metaphase spreads (Figure 1E).

FISH analysis of FFPE tumors revealed one to approximately six large extended ESR1 signals closely associated with smaller centromere 6 signals in all ERα-positive tumors except one. The sizes of the large signals varied, continuously ranging from the

largest one indistinguishable from “HSR type” signals found *ERBB2*-amplified cancer cells as found in Case 1 (Figure 2A), to those slightly larger than centromere 6 signals. The comparison of adjacent sections alternatively used for FISH and IHC frequently showed that the brightness of the fluorescence signal of ESR1 was correlated to the immunohistochemical intensity of ERα, almost on a nucleus-by-nucleus basis (Figures 2B-E). This correlation was found not only in ERα-positive cancer cells, but also ERα-positive non-neoplastic mammary epithelial cells (Figure 2F and G). In the 28 tumors without ERα expression, no large extended signals of *ESR1* were found (Figure 2H).

In FISH analysis on touch smears from 51 tumors consisting of 38 ERα-positive tumors and 13 negative tumors, large extended signals were exclusively found in ERα-positive tumors (Figures 3A and B); however, generally, their numbers in each tumor decreased with the increase of compact *ESR1* signals compared to FISH on FFPE tissues.

DNase I & RNase A treatments

The tight correlation of the extended signal and ERα expression prompted us to test whether the large extended signals of the *ESR1* gene represented DNA-RNA hybridization. After finishing standard FISH and confirming the ‘HSR-type’ signals, cover slips were removed and the sections were treated with DNase I or RNase A. With RNase A treatment, the sizes of the HSR-type signals became much smaller (Figures 3B and C). When DNase I treatment was performed instead of RNase A, although centromere-specific signals were breached, the extended HSR1 signals were unchanged (Figure 3D). Thus, it is most likely that the extended signals of *ESR1* represent nuclear RNA, probably together with its gene.

We further analyzed whether it is possible to visualize processing events along this gene by FISH, and to estimate the three-dimensional structure of this nuclear RNA. This was done by dual-color FISH using SpectrumGreen™-labeled RP11-450E24 and SpectrumOrange™-labeled RP11-54K4. The latter covers the 3'-end portion of *ESR1* from 166 bases downstream of RP11-450E24. The precise locations of the probes' targets are shown in Figure 4A with references to the UCSC Genome Browser [23] and the Ensemble Genome Browser [24]. As a result, dual-color FISH showed that two large spots of the different fluorescences were found abutting each other. Even when they were coalesced, the two RNA accumulations remained as separate signals and did not intermingle as shown in Figure 4D.

Then, we repeated the FISH on all needle biopsies and touch smears with incubation

by RNase A before hybridization. The results showed that the extended signals of *ESR1* disappeared, and all *ESR1* signals were compact signals smaller than centromere 6, both in biopsy specimens and imprinted cells as shown in Figure 5. We counted copy numbers of *ESR1* and centromere 6 and calculated the ratio of *ESR1* signals/centromere 6 signals (amplification ratio) for approximately 40 nuclei per tumor specimen. In needle biopsies of the 106 tumors, two tumors had an amplification ratio of 2.4, which meets the ASCO criterion of *ERBB2* amplification. The FISH of imprinted cells revealed that each tumor was composed of several fractions with different *ESR1*/centromere 6 signal patterns as shown in Figure 5C. The ESR1/centromere 6 signal patterns found in more than 40% of cancer nuclei were considered as predominant subpopulations and are shown in Table 1. The amplification ratios detected for biopsy specimens of the 51 cases in which both FISH on FFPE tissues and FISH on imprinted cells were performed are also shown in Table 1. Three tumors (Cases 1-3) had predominant subpopulations of cancer cells with an additional one to three *ESR1* signals as shown in Figure 5B; thus, they were considered to be tumors with low-level amplifications. However, in two of the three (Cases 2 and 3) this low-level amplification was not detected by FISH on the biopsy specimens as shown by the amplification ratios of 1.5 and 1.6, respectively.

RP11-62N23 / CEP17™

Gene amplification of *ERBB2* was found in 20 cases (18.9%): all 15 of the 3+ tumors and five of 12 of the 2+ tumors. The 13 cases showed the "HSR type" of *ERBB2* signals, and seven had amplification ratios > 2.2, and one tumor (Case 2) showed unequivocal amplification with a ratio of 2.1. Although RNase A treatment altered the *ESR1* signals considerably, it did not change the FISH results of *ERBB2* as shown in Figure 6.

When ERBB2 positive tumors are defined according to ASCO as those with IHC 3+ staining and/or *ERBB2* gene amplification by FISH, the ERBB2 positivity was negatively correlated with ERα overexpression at a statistically significant level (five of 80 versus 15 of 26) ($\chi^2 = 33.9$, $p = 0.00$).

MLPA analysis

MLPA analysis was successful in all 51 tumors in which fresh surgical materials were obtained. The respective means of the two *ESR1* peak values and four *ERBB2* peak values were calculated and are shown in Table 1 with the results of the FISH and IHC of ERα and ERBB2. No *ESR1* 'amplified' tumors (peak value > 2.0) were found, although a 'gain' of *ESR1* was found in five tumors (Cases 1-5). The three tumors with the

highest peak values (Cases 1-3) were those exhibiting low-level amplification by FISH on imprinted cells. However, two of the three did not meet the ASCO-approved criteria of HER2 amplification, which is "the ratio of gene signals per the centromeric signals > 2.2". *ERBB2* 'amplification' was found in six (Cases 9, 27, 33, 34, 41, and 48 in Table 1) by MLPA, and all of them also showed gene amplification by FISH. Among the five tumors with a 'gain' in MLPA (Cases 1, 2, 6, 10, and 31), the one with the highest value (Case 2) showed equivocal amplification by FISH.

Discussion

Gene amplification in small chromosomal regions may appear cytogenetically as HSR and is recognized as a clustered signal in interphase FISH. Conversely, a clustered arrangement of gene signals observed in interphase FISH indicates gene amplification in HSRs; thus, we and others suggest that it should be called "HSR-type" and that it be considered a criterion of gene amplification in FISH analysis of *ERBB2* status [3, 21, 22]. In the present FISH study, variously extended *ESR1* signals were found in ERα-expressing cells. Some of them were indistinguishable from 'HSR-type' signals of *ERBB2* found in breast cancers, and could be considered to represent gene amplification in HSRs. In fact, in previous studies reporting that gene amplification of *ESR1* occurs in more than 20% of breast cancers, these FISH images seem to be the basis for their high reported frequencies [3, 8]. However, the present study showed that this 'HSR-like' signal is RNase A-sensitive and DNase I-resistant; thus, the hybridization partner proved to be RNA.

Concentrations of nuclear RNAs are found by FISH at the transcription sites of such actively transcribed genes as collagen type 1, [25, 26], β-actin [27], and dystrophine [28], and are studied in normal and mutant cells to discern the interrelationship of RNA metabolism and nuclear structure [25, 26]. At the present time, two possibilities that are not mutually exclusive explain nuclear RNAs found by FISH: one is that mRNA forms a "track" that moves away from the gene [26], and the other is that nascent transcripts are attached to the gene-like "trees" [28]. In this respect, our FISH results using two differently labeled probes corresponding to the non-overlapping 5' and 3'-end portions of the *ESR1* gene are very informative, because the two fluorescences representing two portions were not mixed, but were found abutting each other. If the accumulated RNAs were mature mRNAs, then due to their much reduced sizes (less than one forty-fifth)

compared to that of the gene, the signals would have been much weaker, and furthermore, the assembly of molecules containing two portions simultaneously would have made the two color signals intermingle as depicted in Figure 4A. Therefore, our results strongly suggest that the RNA represents newly synthesized nascent RNA molecules extending from the gene as depicted in Figure 4B. It is also possible that this RNA is derived from another gene being transcribed in the opposite direction. For example, it is known that a stable transcript produced from *NCYM*, *MYCN* anti-sense DNA, is cotranscribed with *MYCN* [29]. By searching databases, we found a 258-base transcript [30] that is located on the opposite DNA strand of *ESR1*. However, it is not possible that this small transcript caused the HSR-like signals found in this study.

Unfortunately, FISH analysis using clinical specimens does not have high enough resolving power to further clarify the molecular kinetic events. Smith et al. reported that simultaneous hybridization of differently labeled probes for different non-overlapping sequences within the dystrophine gene, as in our experiment, produced non-overlapping fluorescences in a single-molecular FISH study [28]. They explained the result by 'cotranscriptional splicing', that is, more 5' introns are spliced out of the nascent RNA molecules before the 3' end of the RNA is transcribed; thus, the two sequences of the transcript do not exist simultaneously. In any case, there was a positive correlation between ERα-overexpression detected by IHC and the amount of this nuclear RNA detected by FISH on a nucleus-by-nucleus basis. Thus, this protein overexpression is thought to come from active RNA transcription from *ESR1* genes, which occurs by a different mechanism than gene amplification.

RNA is most vulnerable to degradation during the usual process of making pathological specimens from surgical materials. In fact, in standard protocols of FISH using FFPE tissues, RNase treatment is not mandatory [31] and is only recommended to reduce background RNA staining in FISH using cultured cells [32]. The core needle biopsies used in the present study minimized the duration of pre-fixative steps, and thus may preserve RNA well. FISH on touch smear specimens had fewer extended signals than those found in FFPE tissues in several cases. This is well explained by the fact that the metacarn fixative does not preserve RNA well [33]. However, in spite of being similarly prepared, and the supposedly active RNA transcription, transcripts of ERBB2 were not detected in ERBB2-overexpressing cells. Therefore, RNA retention probably depends on the properties of individual transcripts [33, 34]. In fact, in our previous DNA-DNA FISH studies targeting *EGFR*, *ERBB2*, and *MYC*, etc., we have never found a case where transcript RNA had a significant effect on interpretations FISH results [18, 22, 35].

When the results of MLPA and two FISH analyses were compared, a gain of *ESR1* was found in five tumors by MLPA (Cases 1-5), and the FISH using imprinted cells revealed that three (Cases 1-3) had additional copies of *ESR1*, which were evaluated to be low-level amplification. FISH on FFPE tissues, however, could not detect this low-level amplification in two of them (Cases 2 and 3). This is because FISH on imprinted cells, different from FISH on FFPE tissues, had no effects on nuclear truncation, and thus more precise enumeration of the signals is possible. The sensitivity and specificity of the 'gain' by MLPA against amplification detected by FISH using imprinted cells, if the present cut-off value of 1.3 is used, are 100% and 96%, respectively, and both would be 100% if a cut-off value of 1.4 is used.

In the analysis of *ERBB2*, the six tumors with the highest peak values (Cases 9, 27, 33, 34, 41, and 48) were those with high-level amplification in FISH using FFPE tissues. Both the sensitivity and specificity of MLPA against FISH were 100%. Thus, MLPA is a useful tool to detect gene amplification of *ESR1* and *ERBB2*, especially when an appropriate cut-off value is chosen. Moelans et al. performed MLPA for 135 breast cancers using the same kit and the same analysis software as in the present study, but with DNAs extracted from FEPE tissues, and found gene amplification of *ESR1* in three (2%) with marginal peak values of no more than 2.1 and a gain in 8 (6%) [11]. We do not consider our *ESR1* gain rate of 5.9% (3/51) to be fundamentally different from the frequency of Moelans et al. This low-level amplification was not correlated with ERα overexpression, which mostly occurs by a different mechanism than gene amplification.

Consequently, the consistent results of IHC, FISH, and MLPA in the present study show that the amplification of *ESR1* in breast carcinoma occurs as low-level amplification, and in addition, at a low frequency of 5.9%. We believe that the results in our present study settle the long-standing debate concerning gene amplification of *ESR1* in breast carcinoma.

Acknowledgements

We gratefully acknowledge helpful discussions with Dr. Shin-ichi Horike, Frontier Science Organization, Institute for Gene Research, Kanazawa University; and with Dr. Takeo Kubota, Department of Epigenetic Medicine, University of Yamanashi.

This work was financially supported by the Japanese Ministry of Education, Sports, Science and Culture Nos. C22590310 (A. O.) and C23590409 (Y.D), and The Smoking Research Foundation (Y.D).

Statement of author contributions

AO, MI, JI, YD conceived and designed the work. AO, SH, SK, HI, HK, and RT carried out experiments and analyzed data. All authors were involved in writing the paper and had final approval of the submitted and published version.

Figure legends

Fig. 1

Dual-color FISH using an *ESR1*-specific probe (RP11-450E24, orange fluorescence) and centromere 6-specific probe (green fluorescence) on metaphase spreads of normal bone marrow cells (A) and MCF-7 (E), and interphase nuclei of MCF-7 (B), UACC-812 (C), and MDA-361 (D).

Fig. 2

Dual-color FISH using an *ESR1*-specific probe (RP11-450E24, orange fluorescence) and centromere 6-specific probe (green fluorescence) (A, C, E, G, and H) and IHC for ERα (B, D, and F) on formalin-fixed paraffin-embedded tumors. B and C, D and E, and F and G are adjacent sections alternatively used for FISH and IHC. The same nuclei are denoted by arrows in B and C. The regions within the black rectangle in panels D and F correspond to the fields in panels E and G, respectively. Large 'HSR-like' signals were found in cancer nuclei in A (Case 1), C, and E, and nuclei of ductal epithelia in G. ERα-negative cancer cells have small contracted signals (H).

Fig. 3

Dual-color FISH using an *ESR1*-specific probe (RP11-450E24, orange fluorescence) and centromere 6-specific probe (green fluorescence) on touch smears from Case 1 (A) and Case 10 (B-D). Most *ESR1* signals were 'HSR-like' (A and B). By RNase A-treatment, the ESR1-signals became faint; however, centromere 6 signals were unchanged (C). By DNA-1 treatment, the ESR1-signals were unchanged; however, centromere 6 signals disappeared (D). Panels B and C show the same imprinted cells before and after RNase A treatment.

Fig. 4

Dual-color FISH on imprinted cells using RP11-450E24 (green fluorescence) and RP11-54K4 (orange fluorescence) corresponding to the non-overlapping 5'- and 3'-end portion of *ESR1*, respectively. The precise locations of the probe targets are shown in A, where italic figures represent chromosome position according to the UCSC Genome Browser [23]. The information for the ESR1 transcript was obtained from the Ensemble database [24]. The result showed two large spotty signals fused or tightly apposed (D). B and C are two possible molecular events explaining Panel D. Model B shows nascent transcripts extending from the gene. The 5'-end portion may undergo post-transcriptional splicing. Model C shows mRNAs. The real sequence size of the mRNA is one forty-fifth that of the primary transcript in full-length. Closed circles, dotted lines, and solid lines represent exons and transcripts with and without splicing. Light green and orange areas represent images of fluorescence derived from the two probes, respectively.

Fig. 5

Dual-color FISH using an *ESR1*-specific probe (RP11-450E24, orange fluorescence) and centromere 6-specific probe (green fluorescence) after RNase A treatment on a biopsy specimen (A, Case 1) and imprinted cells (B, Case 1; C, Case 10). HSR-like signals were not found. Compare Panels A, B, and C with Figures 2A, 3A, and 3B, respectively.

Fig. 6

FISH using an *ERBB2*-specific probe (orange fluorescence) and centromere 17-specific probe (green fluorescence) without (A) and with (B) RNase A treatment. The 'HSR-like' signals showed no changes with RNase treatment.

References

1. Allred DC. Issues and updates: evaluating estrogen receptor-alpha, progesterone receptor, and HER2 in breast cancer. *Mod Pathol* 2010; 23 Suppl 2: S52-59.

2. Bedard PL, Piccart-Gebhart MJ. Progress in tailoring adjuvant endocrine therapy for postmenopausal women with early breast cancer. *Curr Opin Oncology* 2009; 21: 491-498.

3. Holst F, Stahl PR, Ruiz C, *et al.* Estrogen receptor alpha (ESR1) gene amplification is frequent in breast cancer. *Nat Genet* 2007; 39: 655-660.

4. Brown LA, Hoog J, Chin SF, *et al.* ESR1 gene amplification in breast cancer: a common phenomenon? *Nat Genet* 2008; 40: 806-807

5. Reis-Filho JS, Drury S, Lambros MB, *et al.* ESR1 gene amplification in breast cancer: a common phenomenon? *Nat Genet* 2008; 40: 809-810.

6. Horlings HM, Bergamaschi A, Nordgard SH, *et al.* ESR1 gene amplification in breast cancer: a common phenomenon? *Nat Genet* 2008; 40: 807-808.

7. Vincent-Salomon A, Raynal V, Lucchesi C, *et al.* ESR1 gene amplification in breast cancer: a common phenomenon? *Nat Genet* 2008 Jul; 40: 809.

8. Tomita S, Zhang Z, Nakano M, *et al.* Estrogen receptor alpha gene ESR1 amplification may predict endocrine therapy responsiveness in breast cancer patients. *Cancer Sci* 2009; 100: 1012-1017.

9. Adelaide J, Finetti P, Charafe-Jauffret E, *et al.* Absence of ESR1 amplification in a series of breast cancers. *Int J Cancer* 2008; 123: 2970-2972.

10. Nielsen KV, Ejlertsen B, Muller S, *et al.* Amplification of *ESR1* may predict resistence to aduvant tamoxifen in postmenopausal patients with hormone receptor positive breast cancer. *Breast Cancer Res Treat* 2011; 127: 345-355

11. Moelans CB, Monsuur HN, de Pinth JH, *et al.* ESR1 amplification is rare in breast cancer and is associated with high grade and high proliferation: a multiplex ligation-dependent probe amplification study. *Anal Cell Pathol* 2010; 33: 13-18.

12. Bunyan DJ, Eccles DM, Sillibourne J, *et al.* Dosage analysis of cancer predisposition genes by multiplex ligation-dependent probe amplification. *Brit J Cancer* 2004; 13: 1155-1159.

13. Moelans CB, de Weger RA, van Blokland MT, *et al.* HER-2/neu amplification testing in breast cancer by multiplex ligation-dependent probe amplification in comparison with immunohistochemistry and in situ hybridization. *Cell Oncol* 2009; 31: 1-10.

14. Kobayashi M, Kawashima A, Mai M, *et al.* Analysis of chromosome 17p13 (p53 locus) alterations in gastric carcinoma cells by dual-color fluorescence in situ hybridization. *Am J Pathol* 1996; 149: 1575-1584.

15. Subik K, Lee JF, Baxter L, *et al.* The Expression Patterns of ER, PR, HER2, CK5/6, EGFR, Ki-67 and AR by Immunohistochemical Analysis in Breast Cancer Cell Lines. *Breast Cancer* 2010; 4: 35-41.

16. Kaplan PA, Frazier SR, Loy TS, *et al.* 1D5 and 6F11: An immunohistochemical comparison of two monoclonal antibodies for the evaluation of estrogen receptor status in primary breast carcinoma. *Am J Clin Pathol* 2005; 123: 276-280.

17. Wolff AC, Hammond ME, Schwartz JN, *et al.* American Society of Clinical Oncology/College of American Pathologists guideline recommendations for human epidermal growth factor receptor 2 testing in breast cancer. *J Clin Oncol* 2007; 25: 118-145.

18. Ooi A, Takehana T, Li X, *et al.* Protein overexpression and gene amplification of HER-2 and EGFR in colorectal cancers: an immunohistochemical and fluorescent in situ hybridization study. *Mod Pathol* 2004; 17: 895-904.

19. Leung KN, Vallero RO, DuBose AJ, *et al*. Imprinting regulates mammalian

snoRNA-encoding chromatin decondensation and neuronal nucleolar size. *Hum Mol Genet* 2009 15; 18: 4227-4238.

20. Coffa J, van de Wiel MA, Diosdado B*, et al.* MLPAnalyzer: data analysis tool for reliable automated normalization of MLPA fragment data. *Cell Oncol* 2008; 30: 323-335.

21. Ishikawa T, Kobayashi M, Mai M, *et al*. Amplification of the c-erbB-2 (HER-2/neu) gene in gastric cancer cells. Detection by fluorescence in situ hybridization. *Am J Pathol* 1997; 151: 761-768.

22. Nakazawa K, Dobashi Y, Suzuki S*, et al.* Amplification and overexpression of c-erbB-2, epidermal growth factor receptor, and c-met in biliary tract cancers. *J Pathol* 2005; 206: 356-65.

23. UCSC Genome Browser on Human Feb. 2009 (GRCh37/hg19) Assembly. ESR1: Available from:http://genome.ucsc.edu/

24 Ensemble Genome Browser 64: Homo sapiens-transcript summary- Transcript: ESR1;ESR1-001:Available from http//www.ensembl.org/ Homo_sapiens/Transcript/

25. Xing Y, Johnson CV, Moen PT, Jr., *et al*. Nonrandom gene organization: structural arrangements of specific pre-mRNA transcription and splicing with SC-35 domains. *J Cell Biol* 1995; 131: 1635-1647.

26. Johnson C, Primorac D, McKinstry M*, et al.* Tracking COL1A1 RNA in osteogenesis imperfecta. splice-defective transcripts initiate transport from the gene but are retained within the SC35 domain. *J Cell Biol* 2000; 150: 417-432.

27. Femino AM, Fay FS, Fogarty K, *et al*. Visualization of single RNA transcripts in situ. *Science* 1998; 280: 585-90.

28. Smith KP, Moen PT, Wydner KL, *et al*. Processing of endogenous pre-mRNAs in association with SC-35 domains is gene specific. *J Cell Biol* 1999; 144: 617-29.

29. Armstrong BC, Krystal GW. Isolation and characterization of complementary DNA for N-*cym*, a gene encoded by the DNA strand opposite to N-*myc*. *Cell Growth Differ* 1992;3:385-90.

30. Vega genome browser 44: Homo sapiens-Gene summary-Gene: RP3-443C4.2 (OTTHUMG00000016436): Available from http://vega.sanger.ac.uk/

31. Squire JA, Marrano P, Kolomietz E. FISH in clinical cytogenetics. In *FISH A practical approach*. Beatty B, Mai S, Squire J (eds). Oxford University Press: New York, 2002; 183-203

32. Beatty BG, Scherer SW. Human chromopsome mapping of single copy genes. In *FISH A practical approach*. Beatty B, Mai S, Squire J (eds). Oxford University Press: New York, 2002; 29-54.

33. Lawrence JB, Singer RH. Intracellular localization of messenger RNAs for cytoskeletal proteins. *Cell* 1986; 45: 407-415.

34. Clemson CM, McNeil JA, Willard HF, *et al*. XIST RNA paints the inactive X chromosome at interphase: evidence for a novel RNA involved in nuclear/chromosome structure. *J Cell Biol* 1996; 132: 259-275.

35. Hara T, Ooi A, Kobayashi M, *et al.* Amplification of c-myc, K-sam, and c-met in gastric cancers: detection by fluorescence in situ hybridization. *Lab Invest* 1998; 78: 1143-1153.

Table 1. Results of MLPA, FISH and IHC analyses of ESR1 and ERBB2

	ESR1				ERBB2		
Case No	MLPA Peak values	Predominant Types ESR1/centromere 6	Paraffin FISH ESR1/CEP6	IHC[a]	MLPA Peak values	Paraffin FISH ERBB2/CEP17	IHC[b]
1	1.78	5/2, 6/3	2.4	2+	1.38	0.82	−
2	1.65	6/4	1.5	2+	1.92	2.1	2+
3	1.46	3/2	1.6	2+	1.15	1.2	−
4	1.35	3/3, 4/4	1.1	2+	1.07	1.4	−
5	1.31	2/2	1.1	2+	0.88	0.89	−
6	1.28	3/3	1,1	2+	1.40	1.3	1+
7	1.26	6/6, 5/5	1.1	2+	1.01	1.3	−
8	1.24	2/2	0.72	2+	1.22	0.99	−
9	1.23	4/4	1.1	2+	4.43	3.9	3+
10	1.17	4/4	1.0	2+	1.40	1.2	2+
11	1.17	2/2	0,99	−	1.16	0.87	−
12	1.17	2/2	1.1	2+	1.20	1.6	−
13	1.15	2/2	1.1	2+	1.07	1.2	−
14	1.13	2/2	1.2	1+	1.14	1.3	−
15	1.11	2/2,4/4	0.92	−	1.00	0.95	−
16	1.11	2/2	0.97	2+	1.19	1.3	−
17	1.11	2/2	1.0	2+	1.14	1.4	−
18	1.11	2/2, 4/4	0.98	−	1.00	0.98	−
19	1.09	2/2	1.0	2+	1.14	1.3	−
20	1.09	6/6,3/3	1.2	1+	1.10	0.82	−
21	1.08	1/2	0.85	−	1.10	1.4	−
22	1.08	2/2	0.88	2+	1.11	1.4	2+
23	1.07	2/2	1.2	−	1.07	1.0	−
24	1.07	2/2	1.1	2+	1.02	0.99	−
25	1.07	2/2	0.99	2+	1.06	1.4	−
26	1.07	2/2,4/4	1.1	−	1.00	0.91	−
27	1.05	5/5	1.1	1+	2.02	HSR	2+
28	1.04	2/2	1.4	2+	1.06	0.99	−
29	1.03	2/2,3/3	1.2	2+	1.07	0.99	−
30	1.03	2/2	1.0	2+	1.09	1.2	−
31	1.02	2/2	1.1	2+	1.91	1.0	2+
32	1.01	4/4,2/2	1,1	2+	1.03	0.89	−
33	1.00	2/2, 4/4	0.98	−	5.86	HSR	3+
34	1.00	2/2	0.99	−	2.42	HSR	2+
35	0.99	3/3	0.89	2+	1.25	1.0	−
36	0.99	2/2	0.99	2+	1.04	1.4	−
37	0.99	3/5, 2/4	0.78	1+	1.07	1.3	−
38	0.99	2/2	1.0	2+	1.05	1.2	−
39	0.97	3/3	1.1	2+	0.92	1.3	−
40	0.96	2/2	1.0	2+	0.87	1.0	−
41	0.95	2/3	0.88	−	13.1	4.6	2+
42	0.95	3/3	1.1	2+	0.99	1.6	1+
43	0.93	3/3	1.0	2+	1.10	0.88	1+
44	0.92	3/3	1.2	2+	1.19	0.92	−
45	0.89	2/3	0.84	1+	1.01	1.1	−
46	0.80	2/3	0.65	−	1.00	1.5	2+
47	0.78	1/2	1.2	1+	1.03	1.2	−
48	0.74	2/3	0.67	−	12.1	HSR	3+
49	0.73	2/4, 1/2	0.67	−	0.96	1.1	−
50	0.71	1/2	0.79	2+	1.20	1.3	−
51	0.65	1/2	1.1	2+	1.13	0.93	−

IHC[a] ; 2+, positive cells > 80%; +, 80% > positive cells > 10%; −, positive cells < 10%.

IHC[b] ; scored according to the criteria recommended by the American Society of Clinical Oncology for IHC of ERBB2

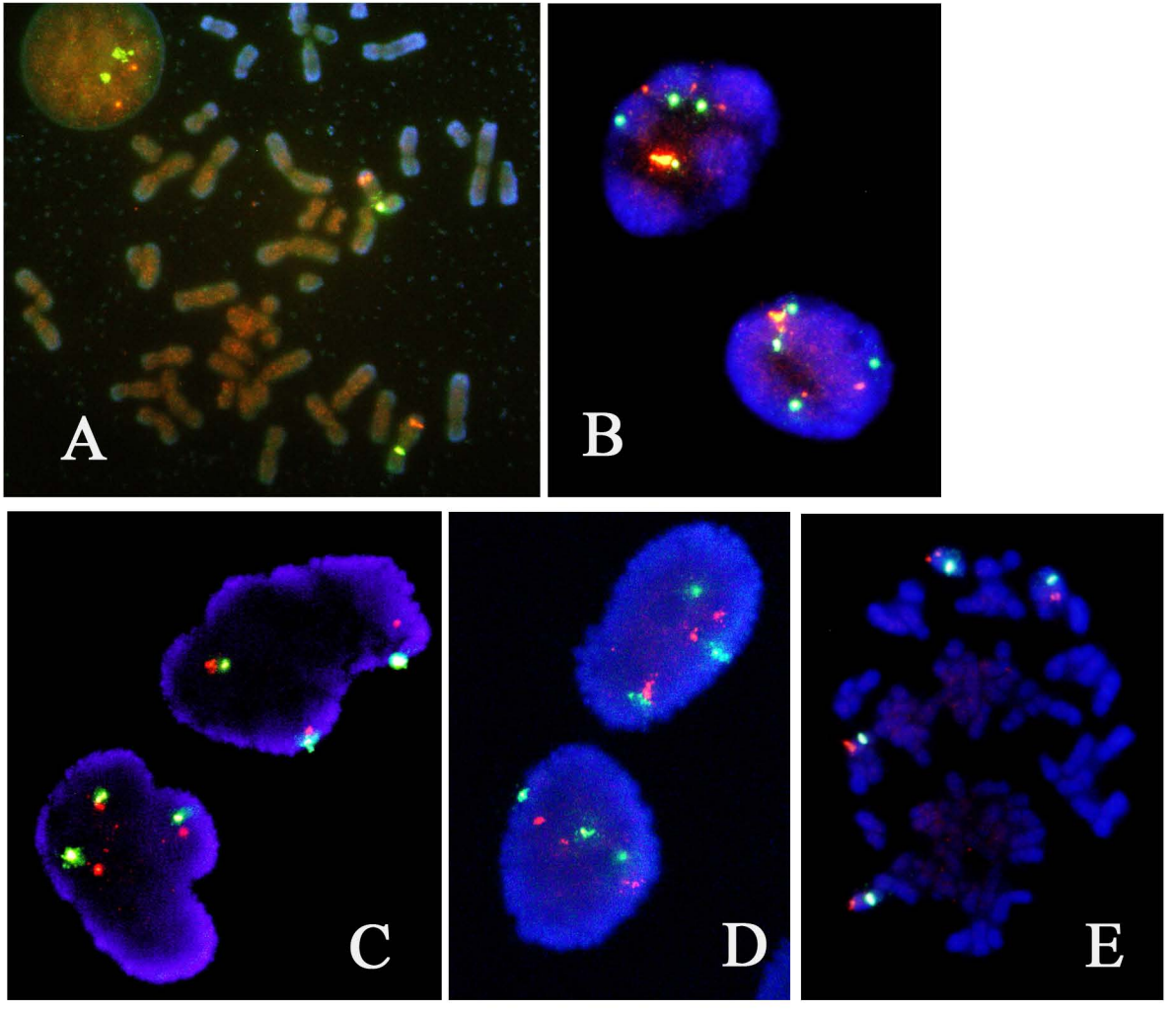
A
B
C
D
E

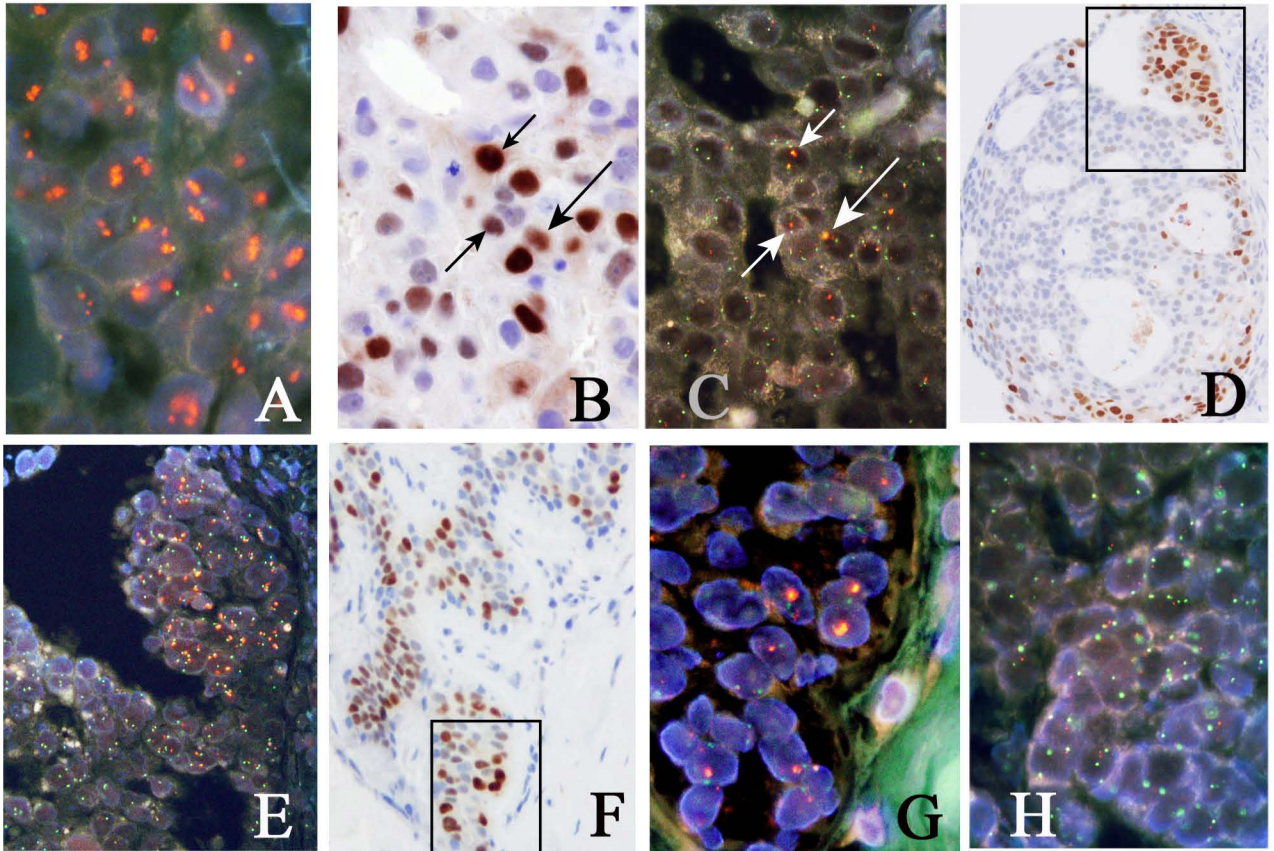
A
B
C
D
E
F
G
H

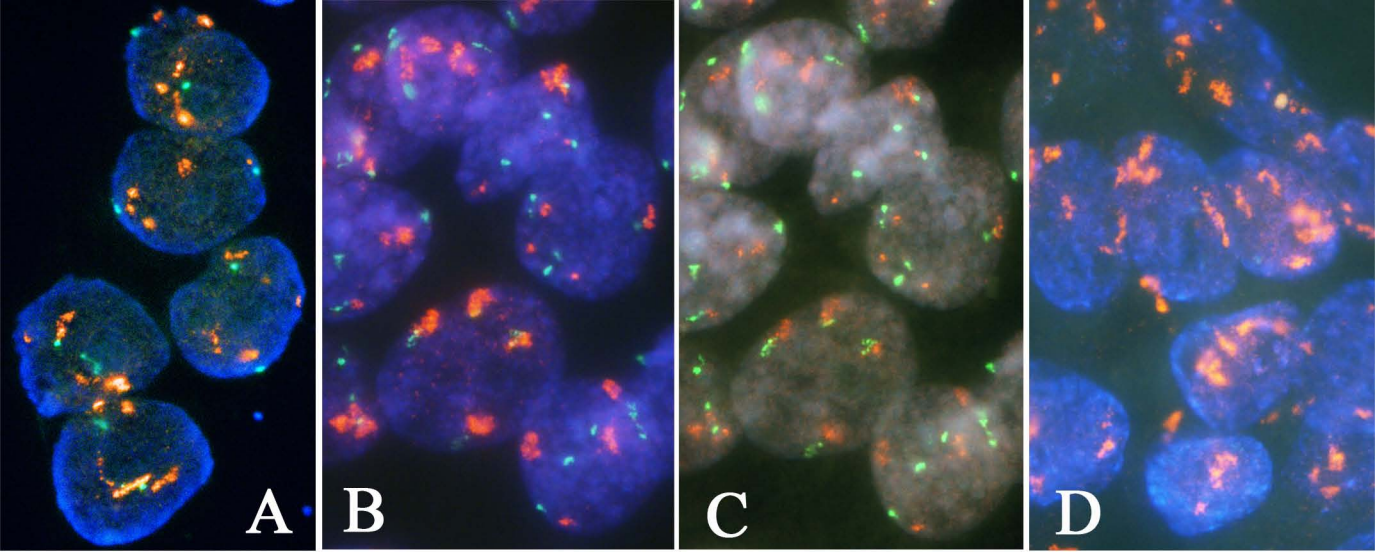
A
B
C
D

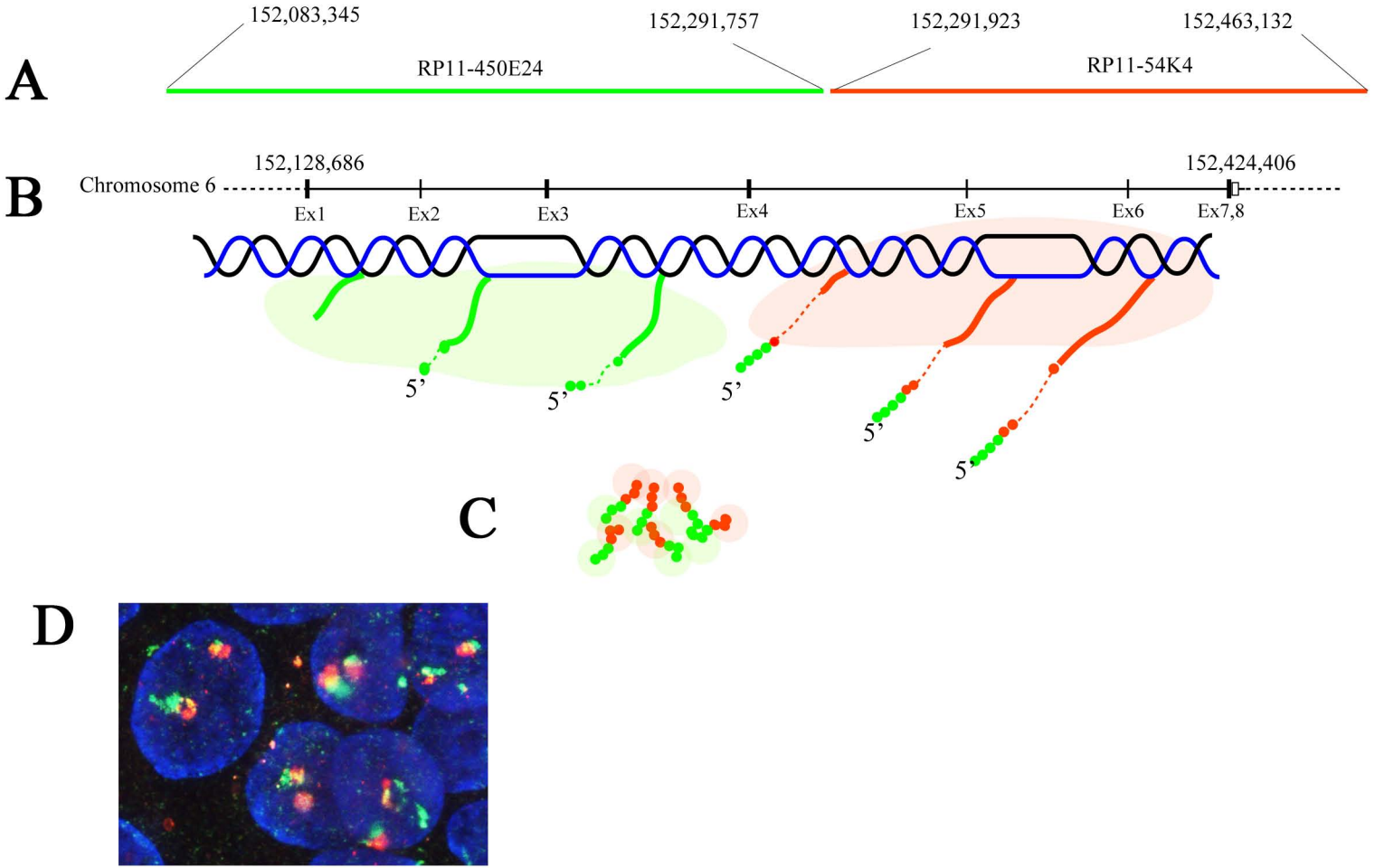
A
152,083,345
152,291,757
152,291,923
152,463,132
RP11-450E24
RP11-54K4
B
152,128,686
152,424,406
Chromosome 6
Ex1
Ex2
Ex3
Ex4
Ex5
Ex6
Ex7,8
5'
5'
5'
5'
5'
C
D